Green Bank Telescope located in West Virginia, U.S.

Spectral Analysis of the North Celestial Pole Loop using ROHSA's multi Gaussian Decomposition

Mukesh Taank, University of Guelph, CITA

Supervisors: Peter G. Martin and Antoine Marchal, CITA

Introduction

Context: In this research, I am studying the North Celestial Pole Loop (NCPL). In this loop, there is evidence of an energetic event, like multiple supernovae explosions or strong winds, that pushed gas out of the disk of the Galaxy. This gas, the neutral interstellar medium (ISM), is generally made of three phases: Cold Neutral Medium (CNM), Unstable Neutral Medium (UNM), and Warm Neutral Medium (WNM).

Goals: I want to understand the impact of this event on the multi-phase thermal structure of the neutral Hydrogen gas (HI). The condensation of CNM structures is a precursor to molecular gas and star formation.

Data and Methods

I am using the GHIGLS HI spectral data from the Green Bank Telescope[2] probes the interstellar structure of Hydrogen (HI) using the 21 cm line. A typical spectrum can be seen in Figure 1.

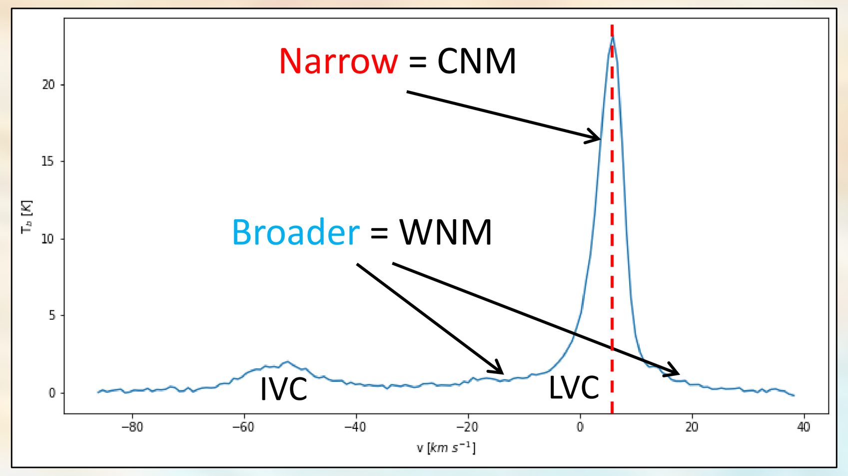

Fig. 1: 21 cm line spectrum for one line of sight in the NCPL. Spectrum plots the brightness temperature [K] at each velocity channel. Red line shows the velocity channel mapped in Figure 2.

These data are stored in a Position-Position-Velocity (**PPV**) cube. The PPV cube has 3 axes: two spatial axes that represent the coordinates on the sky, and the velocity axis that shows the Doppler shifts. A plane in the cube at a fixed velocity maps the brightness temperature across the sky; see example in Figure 2.

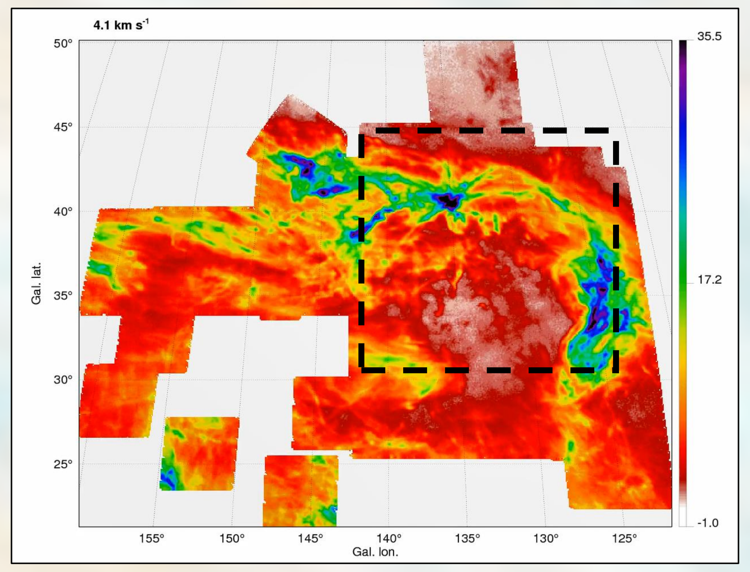

Fig. 2: Brightness temperature [K] map of the NCPL at 4.1 km/s. Black box shows the coverage of the region studied below.

I am analyzing Doppler shifts and the line broadening. The spectral data are **decomposed** with Gaussians by **ROHSA's algorithm**, which introduces **regularization** to obtain a **spatially smooth solution**.

Gaussians with lower velocity dispersion (**sigma**) correspond to colder gas, while those with higher sigma correspond to warmer gas.

Results and Discussion

I ran the ROHSA algorithm to find an optimal decomposition for the data at every velocity channel. The data are fit with 40 Gaussians. I experimented using a different number of Gaussians (n = 32, 40, 48) and different values for the hyper parameters to confirm the stability of the solution.

Key properties of the Gaussians in ROHSA's decomposition are summarized in the two-dimensional histogram of sigma-velocity (σ-v) in Figure 3. This is used to classify the Gaussians into phases.

I have defined **three phases** based on their mean velocity dispersion:

- **CNM** $\sigma < 2.5$ km/s [760 K]
- **UNM** $2.5 \text{ km/s} < \sigma < 5.3$ km/s [3400 K]
- **WNM** $\sigma > 5.3$ km/s

Low and Intermediate Velocity Component regions (**LVC and IVC,** respectively) are defined based on the **morphology** of each component map and their **mean velocity**.

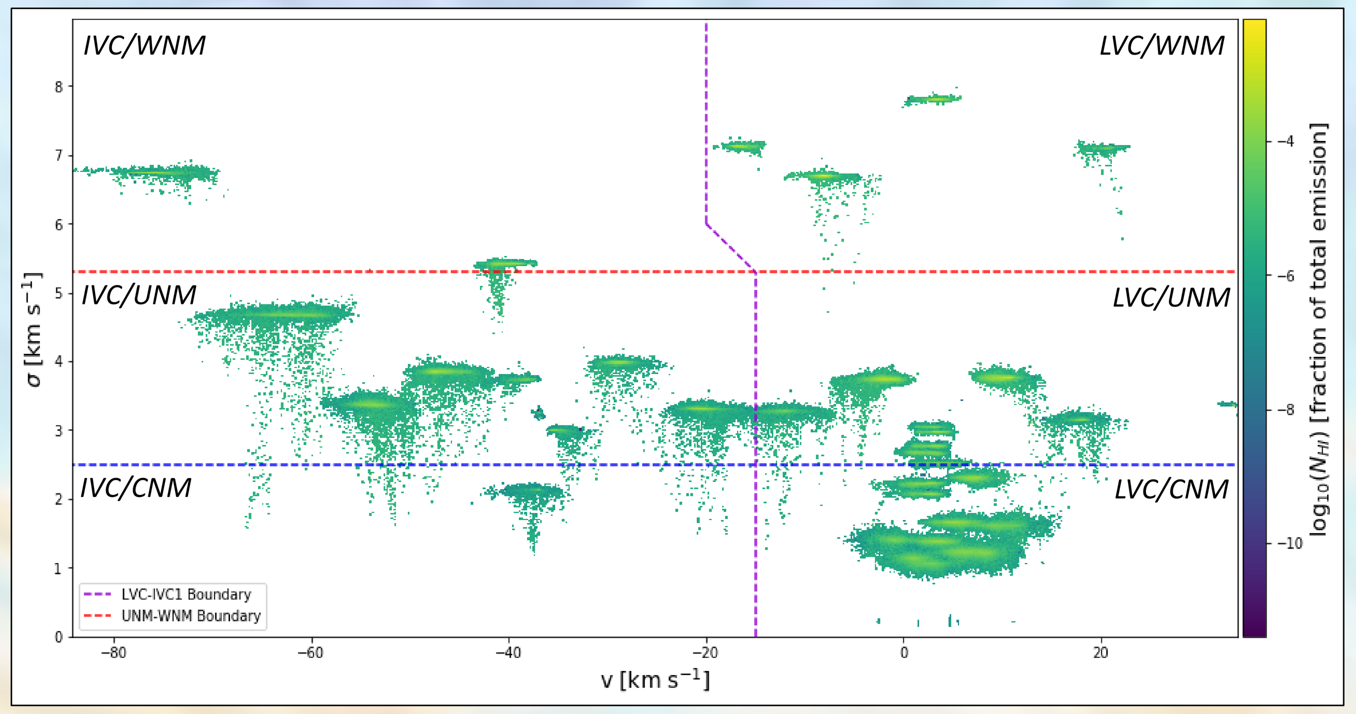

Fig. 3: Two dimensional probability distribution function for σ-v, weighted by the fraction of total emission of each Gaussian

A useful overview of the spatial structure is provided by the **column density (N_{HI})**, which is the integral of the brightness temperature over the velocity. This is shown for the three phases in each velocity range in Figure 4a. For the LVC range, Figure 4b combines these three phases into an RGB image showing their relative weighting.

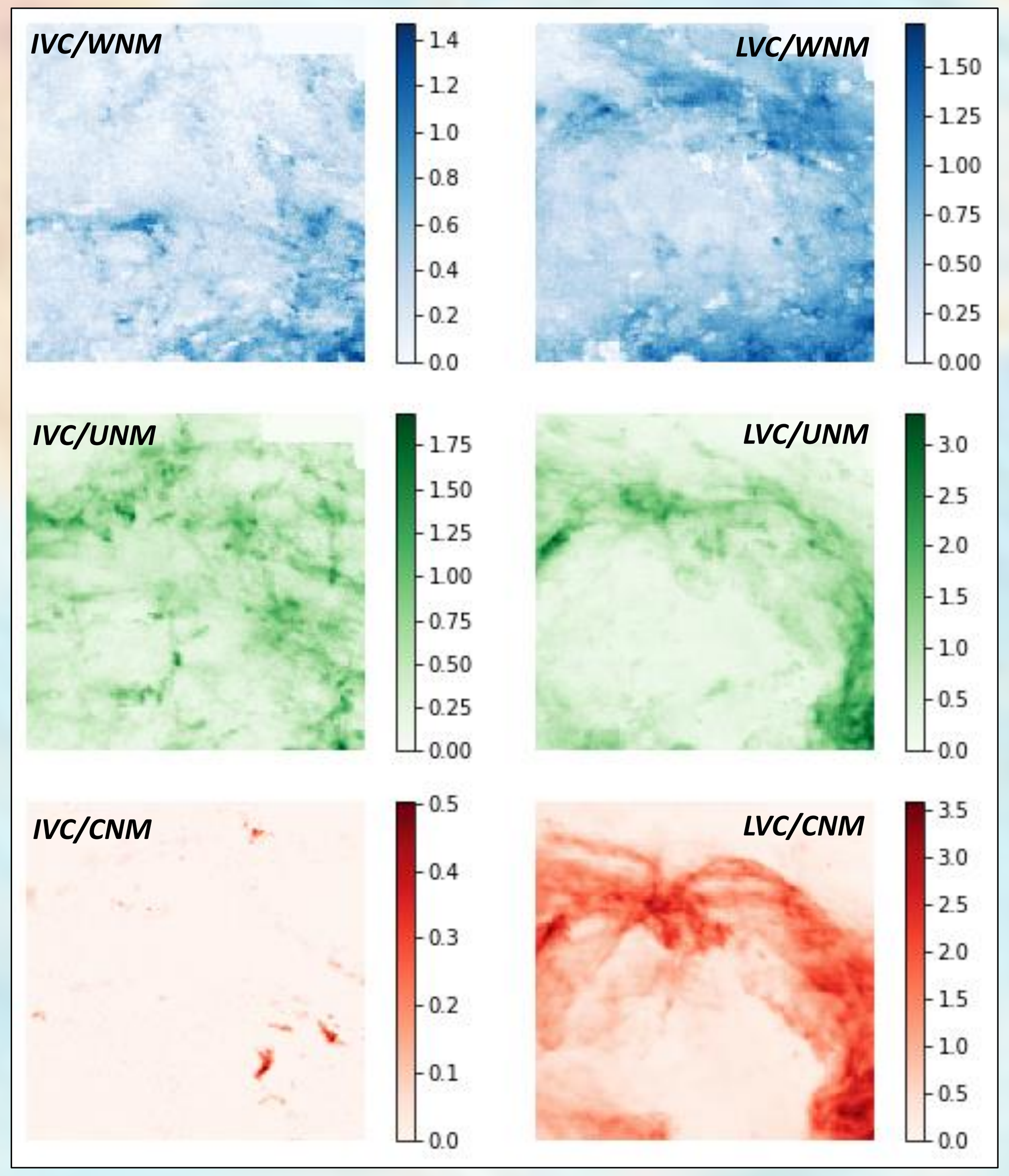

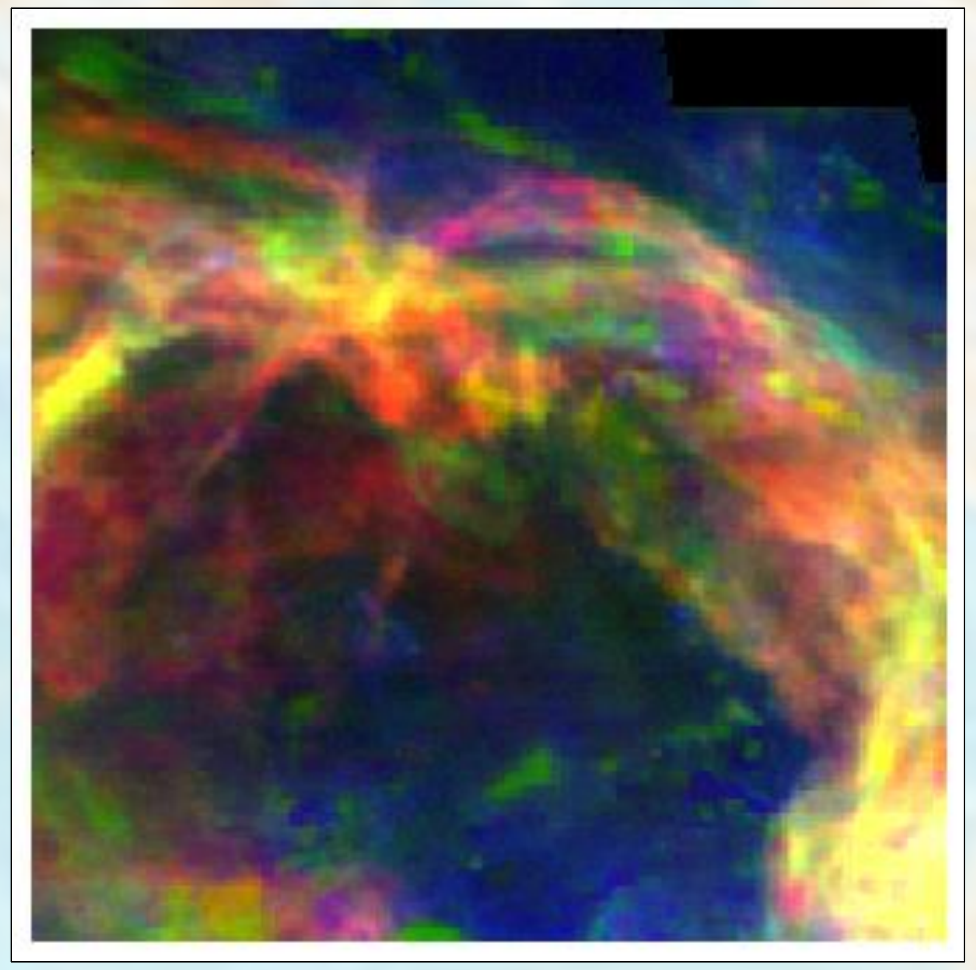

Fig. 4a [left]: Column density maps (NHI/ 10^{20} cm^{-2}) of the phases in the LVC (right) and IVC (left).

Fig. 4b [right]: RGB colour map showing the relative weightings of each phase in the NCPL.

In Figure 4a, the large scale shape of the NCPL can be seen in each phase of the LVC. However, along the loop on a smaller scale, there are anti-correlations between the phases that show that phase transitions have occurred, from warmer to colder gas. For example, at the center of the SPIDER-like structure, I observe a mean CNM and WNM mass fraction of ~80% and ~10%, respectively. Furthermore, in Figure 4b, the predominantly red regions where only CNM is seen suggest that the phase transition is complete. Elsewhere on the loop, the green regions (UNM) indicate that the phase transition is not over. The low density gas on the outskirts of the loop is predominantly blue, i.e., still in the original WNM phase.

Compared to the typical ISM, the NCPL has an unusually large fractional amount of CNM, suggesting that the energetic event was an effective trigger of the phase transition.

Conclusions

In this project, I have been looking at the multi-phase structure of the NCPL, including the SPIDER. I have been studying the phase transition from WNM to CNM.

I have focussed on the Doppler broadening and shifts of the spectral features in the data. This enabled me to examine the multi-phase structure of the NCPL. In the LVC maps of column density, there are anti-correlations that indicate gas that was once present in the WNM is now present in the UNM and CNM. This can only happen by means of a conversion from warmer gas to colder gas.

The energetic event that created the NCPL also triggered this phase transition and led to the unusually large fraction of CNM found along the loop.

Future Prospects

There are many areas of interest that follow from and will complement the original analysis, including:

- Determining the distance and physical size of the NCPL.
- Determining the physical sizes of the CNM structures and the time scale for the phase transition.
- From Planck CO maps, relating the molecular phase to the CNM structures.
- Comparing the gas with the dust thermal emission from Planck (see figure 5).
- From Planck dust polarization, analyzing the magnetic field lines in relation to the gas structures (see figure 5).
- Determining the energetics of the event that led to the formation of the NCPL.

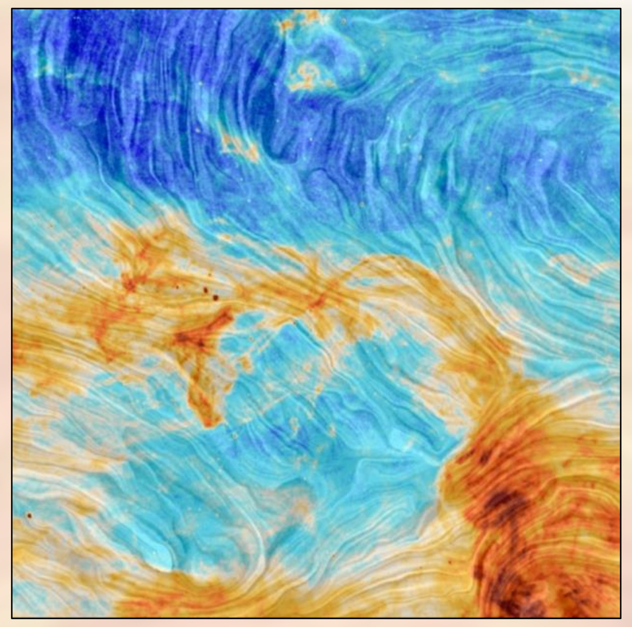

Fig. 5: Intensity of dust emission computed from a combination of Planck observations at 353, 545 and 857 GHz in the NCPL region. The "drapery" pattern indicates the orientation of the magnetic field projected on the plane of the sky, orthogonal to the observed dust polarization.

References

[1] Marchal, A., Miville-Deschênes, M.-A., Orieux, F., Gac, et al. 2019, A&A, 626, A101

[2] Martin, P. G., Blagrave, K. P. M., Lockman, F. J., et al. 2015, ApJ, 809, 153.